Calculation of noise barrier performance using the substitute-sources method for a three-dimensional turbulent atmosphere

Calculation of noise barrier performance using the substitute-sources method for a three-dimensional turbulent atmosphere

Abstract

Substitute sources between a noise barrier and a receiver are used to calculate the effect of atmospheric turbulence on barrier sound reduction. The method is extended for application to three-dimensional situations with both high and low barriers. Calculations are made for a thin, hard screen, without the influence of a ground surface. The Kirchhoff approximation is applied for the low screens and a more accurate diffraction model is used for the higher screens. The calculated results are compared with corresponding ones for two-dimensional situations, by using the substitute-sources method (SSM) also. The two and three-dimensional calculations give very similar results, which indicates that, for a large variety of situations, only two-dimensional models are needed. The results are also compared with those obtained using a scattering cross-section method which, although it predicts a much weaker influence of turbulence than the SSM, shows mostly the same trend, namely that the turbulence influence is large only within a range of lower screen heights.

1. Introduction

This paper describes an extension of the substitute- sources method [1]. The problem under study is the increase in sound level behind barriers due to the influence of atmospheric turbulence on the sound propagation. Screens and buildings along roadsides are used as noise barriers for reducing the traffic noise in residential areas. For an accurate prediction of the performance of noise barriers, the heterogeneous nature of the outdoor air needs to be taken into account. Wind and temperature variations with height determine the mean sound speed profile, and the atmospheric turbulence causes local fluctuations. The turbulence can be seen as causing scattering of sound into acoustic shadow regions behind barriers. Various models can be used to predict this effect. One of these is a scattering cross-section model [2, 3, 4], which uses a single-scattering approximation. The parabolic equation method (PE) can also be used [5], which is suitable for flat geometries, i.e. when the barrier height is not too great in comparison with the distances from the barrier to the source and to the receiver. In the present paper, a substitute-sources method (SSM) was used. This method was previously implemented for two-dimensional (2-D) situations with flat geometries [1, 6]. Here, three-dimensional (3-D) situations are also studied, and results for steep geometries are shown as well. The SSM assumes that the atmosphere is turbulent on only one side of the barrier, hence, it is best suited for situations where the barrier is much closer to the source than to the receiver, or vice versa. The introduction of a ground surface, treated in a previous work [1], was not made here. Also, an implementation with randomised source strengths has been tested [6].

In terms of physical modelling, the problem with a noise barrier in an outdoor environment can be seen as arising from two interacting processes: diffraction (due to the barrier) and sound propagation in an inhomogeneous medium. A direct numerical solution to the whole problem would generally be very expensive

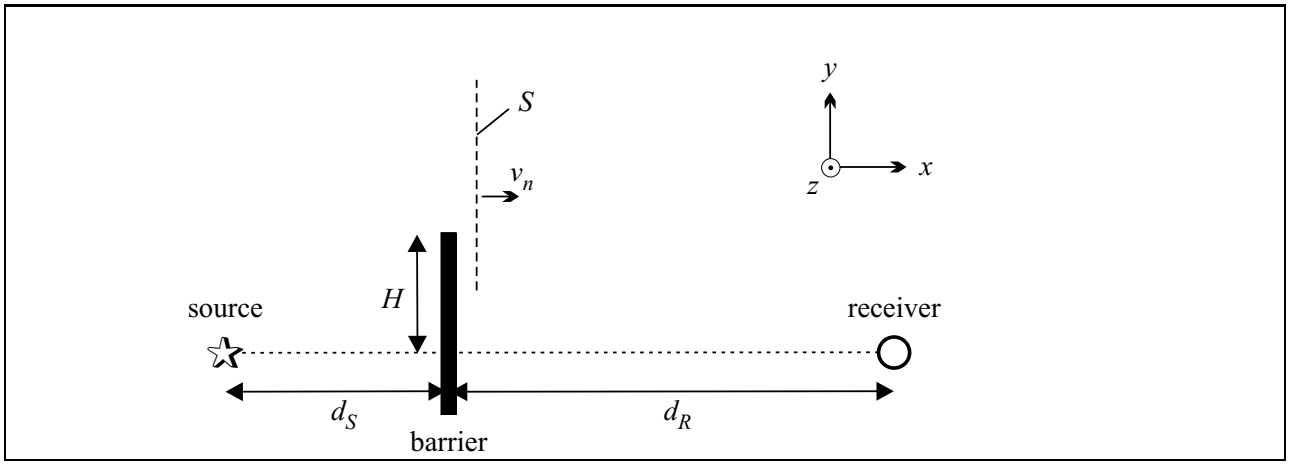

Figure 1. Geometrical situation with source, barrier, receiver, and the substitute surface, S.

computationally (e.g. by using a finite element method), thus, it is preferable to have a model that separates the two processes to some extent, without too large approximations.

The approach is to describe the field of a receiver, reached by sound from an original source, as a superposition of fields from a distribution of sources on a surface located between the original source and the receiver. The surface is denoted the substitute surface, and the sources on it are substitute sources. (See Figure 1.) When the substitute surface is located between the barrier and the receiver, there is a free path from all of the substitute sources to the receiver, and the calculation of the sound propagation along the free path is possible for a variety of situations with an inhomogeneous atmosphere. A mutual coherence function for a turbulent atmosphere has been applied here. Another possibility is to take into account the refraction due to a sound speed profile.

In this model the turbulent atmosphere is assumed to increase the noise level behind the barrier by a decorrelation of the contributions from the substitute sources. This implies that, in the absence of turbulence, the substitute sources must be interfering negatively.

The strengths of the substitute sources are calculated as for a barrier in a homogeneous atmosphere. This approximation would be acceptable for weak inhomogeneity (a weak turbulence) or when the distance from the source to the barrier is much shorter than the total source to receiver distance. (If instead, the distance from the receiver to the barrier is much shorter than the total source to receiver distance, the reciprocal problem should be studied with source and receiver positions interchanged.) In a previous study [1], the Kirchhoff approximation was used, which restricted the work to flat geometries. The results were compared with those from PE calculations. Here, results were calculated for 2-D and 3-D situations, both with and without the Kirchhoff approximation. The results from using the different approaches were compared; a comparison with a scattering cross-section method was also made. The situations studied here are for a thin hard screen, with edge parallel to the z axis and both the source and receiver at $z = 0$.

2. Theory

The theoretical tools needed for the model with substitute sources consist mainly of two types. First, the strengths of the substitute sources need to be determined, i.e. the normal velocity of the sound field at the substitute surface is needed as the source distribution for the Rayleigh integral. Second, at the receiver, the

expected acoustic power of the sum of the signals that have propagated through the turbulent atmosphere from all of the substitute sources needs to be estimated. This is done by calculating the mutual coherence between all substitute sources, using a mutual coherence function (MCF), or transverse coherence function, for a turbulent medium.

2.1. Use of the Rayleigh integral

When the substitute surface (denoted S) is a plane and the particle velocity, v_n, normal to the plain is known, then the monopole source strengths of the substitute sources are known, and the resulting pressure amplitude, p, at the receiver position, $\boldsymbol{x}_R$, can be calculated as a Rayleigh integral:

$$p(\boldsymbol{x}) = \frac{\mathrm{j}\omega\rho_0}{2\pi}\int_S v_n(\boldsymbol{x}_S)G(\boldsymbol{x}_S|\boldsymbol{x})\mathrm{d}S, \tag{1}$$

where $\boldsymbol{x}_S$ is a point on the surface S, ω is the angular frequency of a time-oscillation, $\mathrm{e}^{\mathrm{j}\omega t}$, with time t, ρ_0 the medium density, and G is a Green function. For a homogeneous 3-D free space the Green function can be written

$$G(\boldsymbol{x}_S|\boldsymbol{x}) = \frac{\mathrm{e}^{-\mathrm{j}kR}}{R}, \tag{2}$$

where R is the distance between $\boldsymbol{x}_S$ and $\boldsymbol{x}$, and k is the wave number $k = \omega/c$, with c the sound speed. The free space Green function (equation 2) can be replaced by another Green function if this suits the situation better. For instance, a sound speed gradient that causes a curving of the sound paths can be described by an appropriate Green function, obtained either analytically or numerically.

The normal velocity, v_n, on the surface S can be seen as consisting of two parts: the free field contribution, v_{n0}, and the contribution due to the diffraction from the barrier, v_{nd}:

$$v_n = v_{n0} + v_{nd}. \tag{3}$$

The free field velocity contribution, v_{n0}, can be calculated from the free field pressure, p_0, as

$$v_{n0} = \frac{-1}{\mathrm{j}\omega\rho_0}\nabla p_0 \cdot \boldsymbol{n}, \tag{4}$$

where $\boldsymbol{n}$ is the unit vector normal to the surface S in the direction away from the source. The free field pressure, p_0, can be written

$$p_0(\boldsymbol{x}_S) = \frac{Q}{R_0}\mathrm{e}^{-\mathrm{j}kR_0}, \tag{5}$$

where Q is a source strength and R_0 is the distance from the source to the point $\boldsymbol{x}_S$ on the surface S.

The diffraction contribution, v_{nd}, is obtained using the uniform theory of diffraction (UTD) for the pressure [7, 8]. The velocity at a point on S is calculated from a numerical derivative of the pressure at two points separated by a small space ($\lambda/50$ is used here). The UTD gives an approximate solution with a small error provided the distance to the screen edge is large enough. The exact solution for the velocity has a singularity at the screen edge, which can make the numerical calculations difficult. In the implementation, a shortest space of one wavelength between the screen and S was used, which also makes the UTD applicable [9].

The UTD is used also for the 2-D calculations. It is then assumed that a diffraction calculation method for 2-D problems gives the same solution relative to free field as a 3-D method at $z = 0$ (i.e. in the xy plane that

goes through the source and is perpendicular to the screen edge). In 2-D the free field pressure can be written as the far-field approximation:

$$p_{0,2-D}(\boldsymbol{x}_S) = Q_{2-D}\frac{\pi}{\mathrm{j}}H_0^{(2)}(kR_0) \approx Q_{2-D}\frac{\sqrt{2\pi}}{\sqrt{kR_0}}\mathrm{e}^{-\mathrm{j}(kR_0+\pi/4)}, \tag{6}$$

where the 2-D Green function $G(\boldsymbol{x}_S|\boldsymbol{x})_{2-D} = \pi/\mathrm{j}H_0^{(2)}(kR_0)$ was used. It should be noted that different Green functions could have been chosen; any factor will cancel out later when each result is related to the corresponding free field level. The velocity in 2-D ($v_{n,2-D}$) is then obtained from multiplying v_n by $p_{0,2-D}/p_0 = (Q_{2-D}G_{2-D})/(QG)$. For the calculation of the contribution of $v_{n,2-D}$ to the received pressure, a Rayleigh integral for 2-D should be used, which can be written

$$p_{2-D} = \frac{\mathrm{j}\omega\rho_0}{2\pi}\int_l v_{n,2-D}(y)G_{2-D}(kR)\mathrm{d}y = \frac{\omega\rho_0}{2}\int_l v_{n,2-D}(y)H_0^{(2)}(kR)\mathrm{d}y, \tag{7}$$

where R is the distance from the point y to the receiver and l is the line of integration. In the implementation of equation (7), the far field approximation of the Hankel function is used, as in equation (6).

When the diffraction contribution is omitted, we have the Kirchhoff approximation, i.e. $v_n = v_{n0}$ above the line of sight and zero below. The Kirchhoff approximation was found to give a small error (< 1 dB) for diffraction angles smaller than about 12° in high frequency situations similar to the ones studied here [1]. A diffraction angle of 12° corresponds to a screen height of about 4 m for the geometries studied here.

2.2. Influence of a turbulent atmosphere

There is line of sight propagation from the substitute sources on the surface S to the receiver, that is, no barriers or other obstacles are shielding the sound propagation. For contributions p_i, $i = 1 \ldots N$, from the substitute sources in a turbulent atmosphere, the long-term average of the square of the total pressure amplitude can be computed [10] as

$$\langle|p_{tot}|^2\rangle = \sum_{i=1}^{N}|p_i|^2 + 2\sum_{i=1}^{N-1}\sum_{j=i+1}^{N}|p_ip_j|\cos\left[\arg\left(\frac{p_j}{p_i}\right)\right]\Gamma_{ij}, \tag{8}$$

where Γ_{ij} is the mutual coherence function fulfilling $0 \leq \Gamma_{ij} \leq 1$. The corresponding equation for a continuous source distribution can be written as

$$\langle|p_{tot}|^2\rangle = \langle\iint p(x)p^*(x')dxdx'\rangle = \tag{9}$$

$$\int\int|p(x)p(x')|\cos\left[\arg\left(\frac{p(x')}{p(x)}\right)\right]\Gamma(x,x')\mathrm{d}x\mathrm{d}x',$$

where x and x' are positions on the substitute surface, and where the asterisk, *, stands for the complex conjugate. If there were a homogeneous atmosphere, $\Gamma \equiv 1$, equation (9) could be seen as the square of the Rayleigh integral in equation (1). The quantity $\langle|p_{tot}|^2\rangle$ is proportional to the power of the signal at the receiver.

Now we can calculate the influence of a turbulent atmosphere for our example, in which the effect of a barrier is modelled by a distribution of substitute sources on a surface, S. If the strength of the substitute sources is described by v_n as in equation (1), we get

$$\langle|p_{tot}|^2\rangle = \left(\frac{\omega\rho_0}{2\pi}\right)^2\int_S\int_S|v_nGv_n'G'|\cos\left[\arg\left(\frac{v_n'G'}{v_nG}\right)\right]\Gamma\mathrm{d}S\,\mathrm{d}S', \tag{10}$$

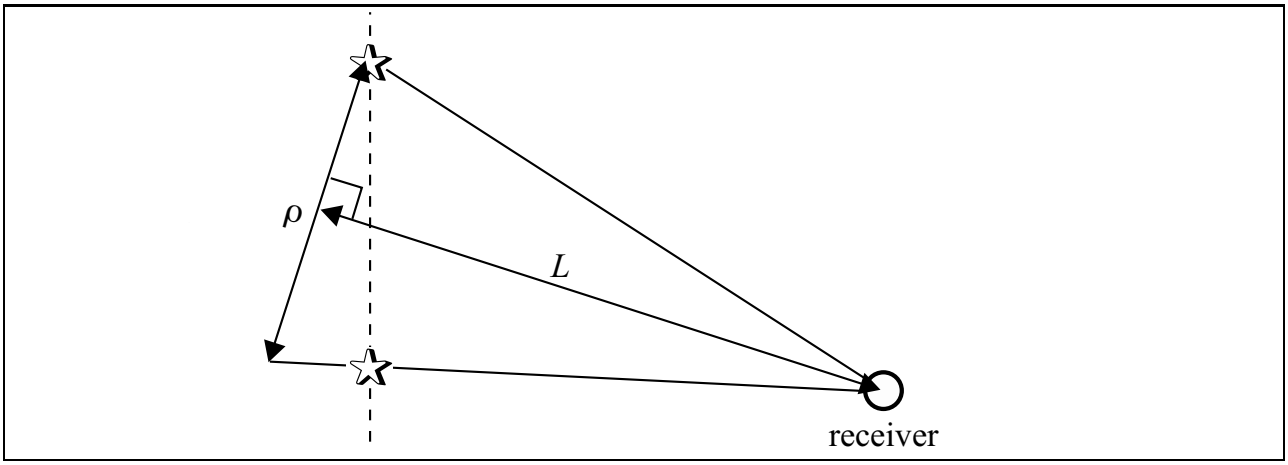

Figure 2. Longitudinal (L) and transversal (ρ) distance for two sources and one receiver.

where $p = p(\boldsymbol{x}), v_n = v_n(\boldsymbol{x}_S), v_n' = v_n(\boldsymbol{x}_S'), G = G(\boldsymbol{x}_S|\boldsymbol{x}), G' = G(\boldsymbol{x}_S'|\boldsymbol{x}), \Gamma = \Gamma(\boldsymbol{x}_S, \boldsymbol{x}_S')$, and dS' refers to $\boldsymbol{x}_S'$, dS refers to $\boldsymbol{x}_S$.

To describe the turbulence, a homogeneous and isotropic turbulence is assumed, that is, the fluctuations are assumed to follow the same statistics for all points and the statistics are independent of rotation. This is a simplified description which could be improved in future work. For the Kolmogorov spectrum of the turbulence, which is used here, the mutual coherence function can be written as

$$\Gamma(L, \rho) = \exp\left[-\frac{3}{8} D \left(\frac{C_T^2}{T_0^2} + \frac{22}{3} \frac{C_v^2}{c_0^2} \right) k^2 \rho^{5/3} L \right], \tag{11}$$

where $D \approx 0.364$, ρ is the transversal distance between the sources and L is the longitudinal distance to the receiver [11, 12]. The strengths of the temperature and the velocity turbulence are given by C_T^2 and C_v^2, respectively; the mean temperature, T_0, is measured in Kelvin, however in this study only velocity turbulence is modelled.

The mutual coherence function (equation 11) is used for both the 3-D and the 2-D calculations. For the 2-D calculations, the values of the input parameters are found from the projections on the vertical xy plane at $z = 0$. The properties of the 2-D turbulence that this corresponds to have not yet been investigated by the author.

When deriving equation (11), the two source positions are assumed to be equidistant from the receiver, while L is the distance from the receiver to the midpoint between the two sources. Here, the two sources are not necessarily the same distance from the receiver, which is why a modification was made. The longest of the two distances was chosen to determine the value of L, as shown in Figure 2. The transversal distance, ρ, forms the base of a triangle, the two other sides of which are of equal length, and whose common angle has the bisector L.

The mutual coherence function can be derived with the parabolic equation and the Markov approximation [13]. Although other approaches besides the parabolic equation can be used [14], it is assumed that the transversal distance, ρ, is small compared with the longitudinal distance, L. In all of the situations studied here, the transversal distances are shorter than the longitudinal distances, and it assumed that the corresponding error is negligible. It is also assumed that the correlation radius, ρ_c, of the sound field is large enough in comparison with the wavelength, i.e. $k\rho_c \gg 1$ [12]. The worst case studied here is for $C_v^2 = 5$ m$^{4/3}$/s^2, $d_R = 200$ m, and for $f = 1000$ Hz, which gives $k\rho_c \approx 10$. (The correlation radius is found from setting $\Gamma = \mathrm{e}^{-1}$.)

In the scattering cross-section method used for the comparison, the scattered power is calculated separately and added to the diffracted power at the receiver [2]. The scattered power is obtained by integrating the scattering cross-section over a volume above the barrier [3, 15]. The scattering cross-section method has previously been evaluated by a comparison with measurements [2, 4].

3. Implementation

The calculations including v_{nd}, i.e. without the Kirchhoff approximation, were made for screen heights $H = 2.5$, 5, 11, 20, 35, and 50 m. With the distance from the source to the screen $d_S = 20$ m, the angles to the screen edge from the horizontal are approximately $7°, 14°, 29°, 45°, 60°$, and $68°$. When using the Kirchhoff approximation, the results for all screen heights are given from a single calculation: starting with the contribution of the sources at $y_{\max}$, the result for a lower screen is found by adding the effect of additional sources below $y_{\max}$.

The maximum height, $y_{\max}$, needed for the substitute sources was obtained from test calculations. It was found that the height needed is much lower for calculations with turbulence than for those without it. This means that when the surface S is enlarged, the convergence is faster with turbulence than without, which is an interesting result and also leads to much shorter computation times. In the calculations for the homogeneous atmosphere, $y_{\max}$ needed to be approximately doubled.

For the 3-D calculations, $y_{\max} = 45$ m was used for all calculations with turbulence, both with and without the Kirchhoff approximation, except for $H = 50$ m where $y_{\max} = 90$ m was used. For the 2-D calculations, a value of $y_{\max}$ around 100 meters was used throughout. For the 3-D calculations, the maximum extension in the positive and negative z directions was given the same value as for $y_{\max}$. The size of the substitute surface was kept to a minimum to get manageable computation times (a few hours on a modern PC for each example), and the error due to the finite surface is of the order of 0.5 dB at the most.

In the 3-D calculations, the free field velocity, v_{n0}, was calculated from the lowest point of the line of sight up to $y_{\max}$. (Since the surface S is separated a small distance from the screen, the lowest point of the line of sight is not at the height of the screen edge, but slightly above.) The velocity due to the diffraction from the barrier, v_{nd}, decays faster with height than v_{n0}, for the situations studied here. The calculation of v_{nd} was made for heights within ± 3 meters from the lowest point of the line of sight for all 3-D situations, except for $H = 50$ m where the corresponding distance was increased to 6 meters. For the 2-D calculations, the distance was 6 meters throughout.

A discretisation distance of $\lambda/5$ was used for all of the calculations. When the integral in equation (8) is discretised it takes the form of the sum in equation (10).

4. Results

In Figure 3 an example of how the power of the received signal can vary with screen height is shown for a turbulent atmosphere (solid line) and a non-turbulent, homogeneous atmosphere (dashed line). When the results are obtained using the Kirchhoff approximation, the 3-D and 2-D curves for a homogeneous atmosphere are identical except for small ripples due to the differences in the discretisation (not visible in the figure). With turbulence the results are very similar (indistinguishable in the figure). For a screen well below the line of sight, (i.e. well below $H = 0$), the solutions with and without turbulence tend towards the free field solution. When increasing the screen height from minus infinity, the effect of the turbulence can be seen as a decrease in

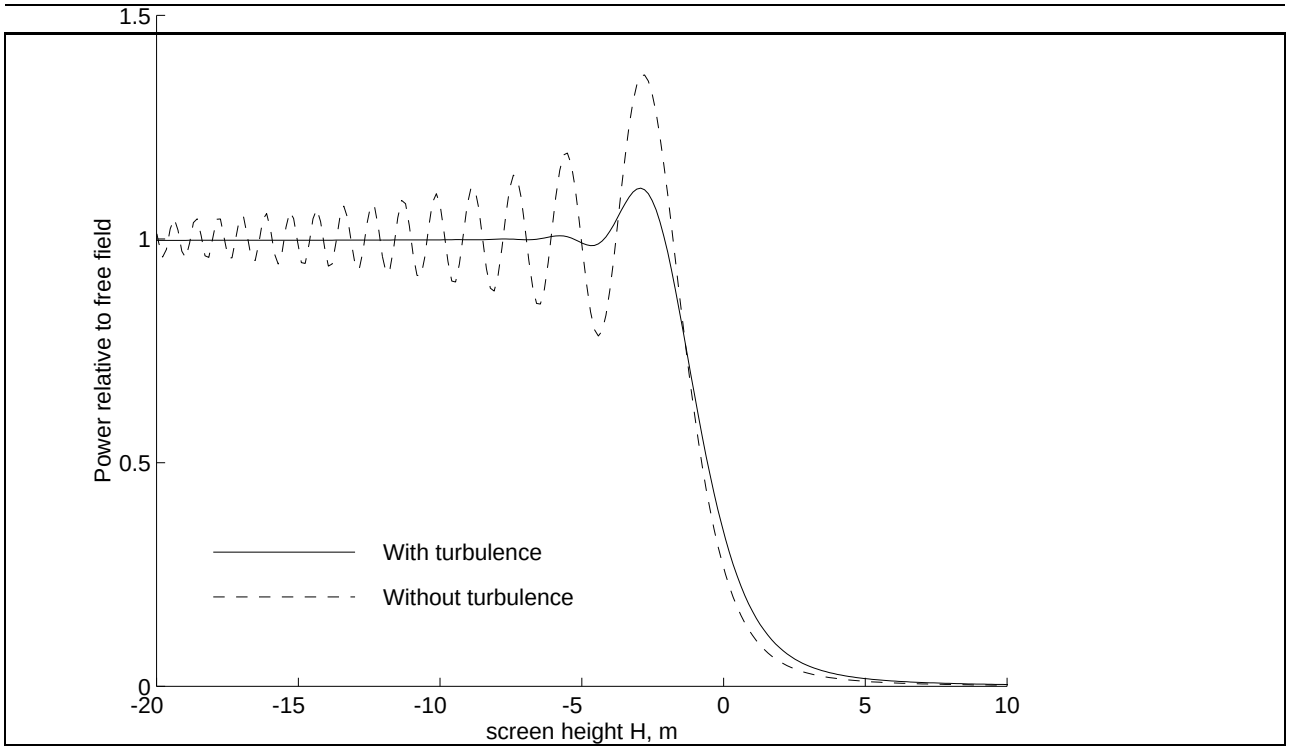

Figure 3. Results for a received signal power variation caused by a changing screen height with and without turbulence (f =500 Hz, d_R =100 m, and C_v^2 =2.5m$^{4/3}$/s^2).

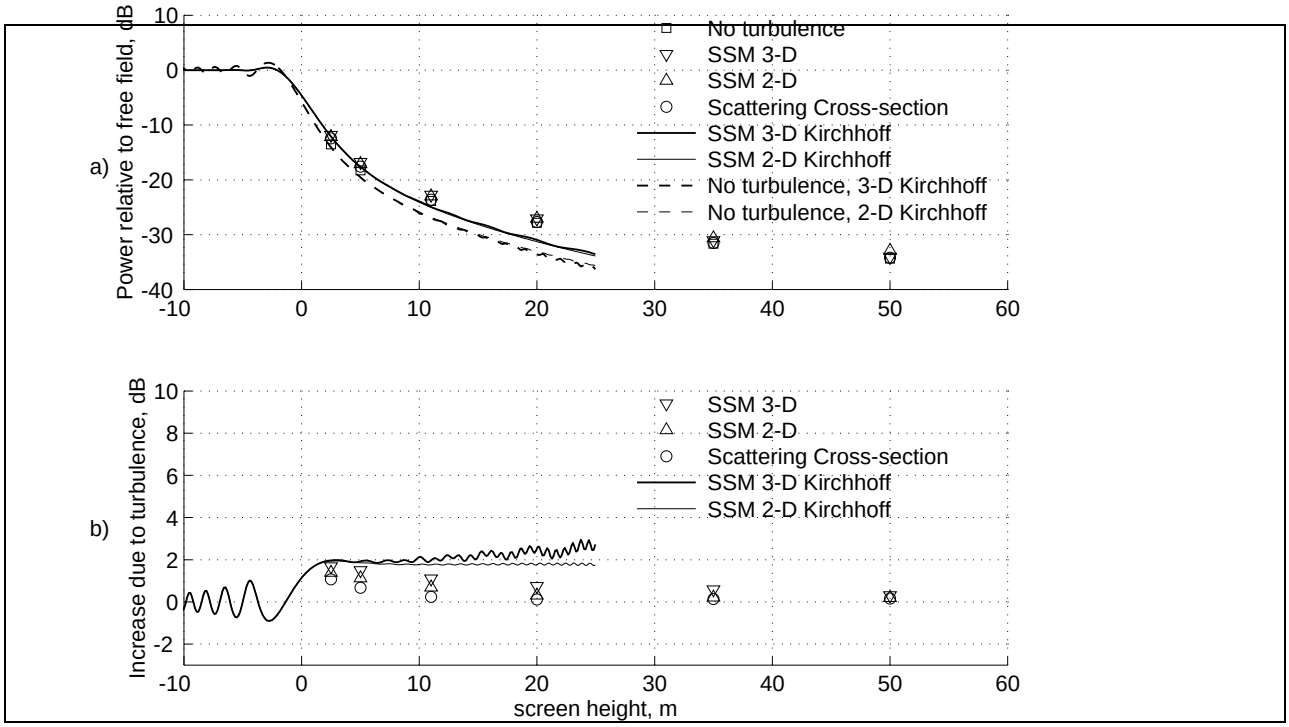

Figure 4. f =500 Hz, d_R =100 m, C_v^2 =2.5m$^{4/3}$/s^2.

the oscillation amplitude. When the screen height approaches zero and increases, the power for the turbulent atmosphere falls off more slowly than for the homogeneous atmosphere. For positive screen heights, there is an increase caused by the turbulence, which is the main effect of interest in this study.

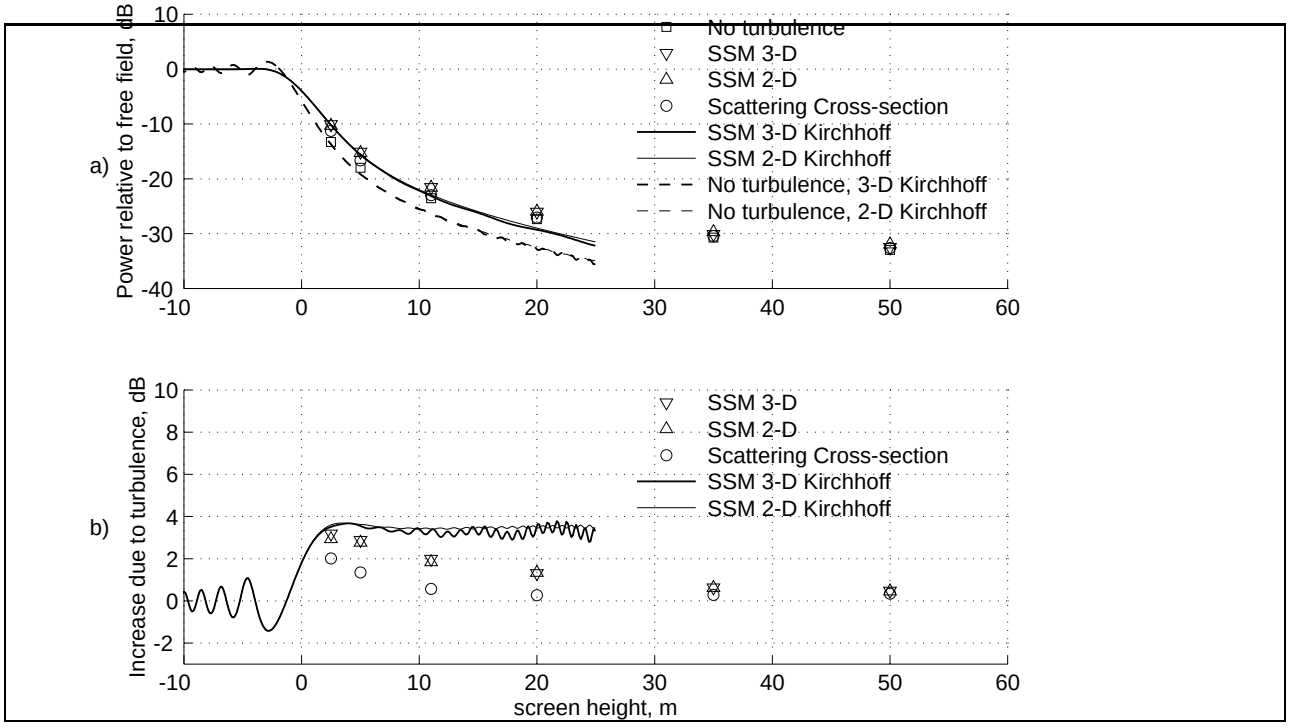

Figure 5. f =500 Hz, d_R =200 m, C_v^2 =2.5m$^{4/3}$/s^2.

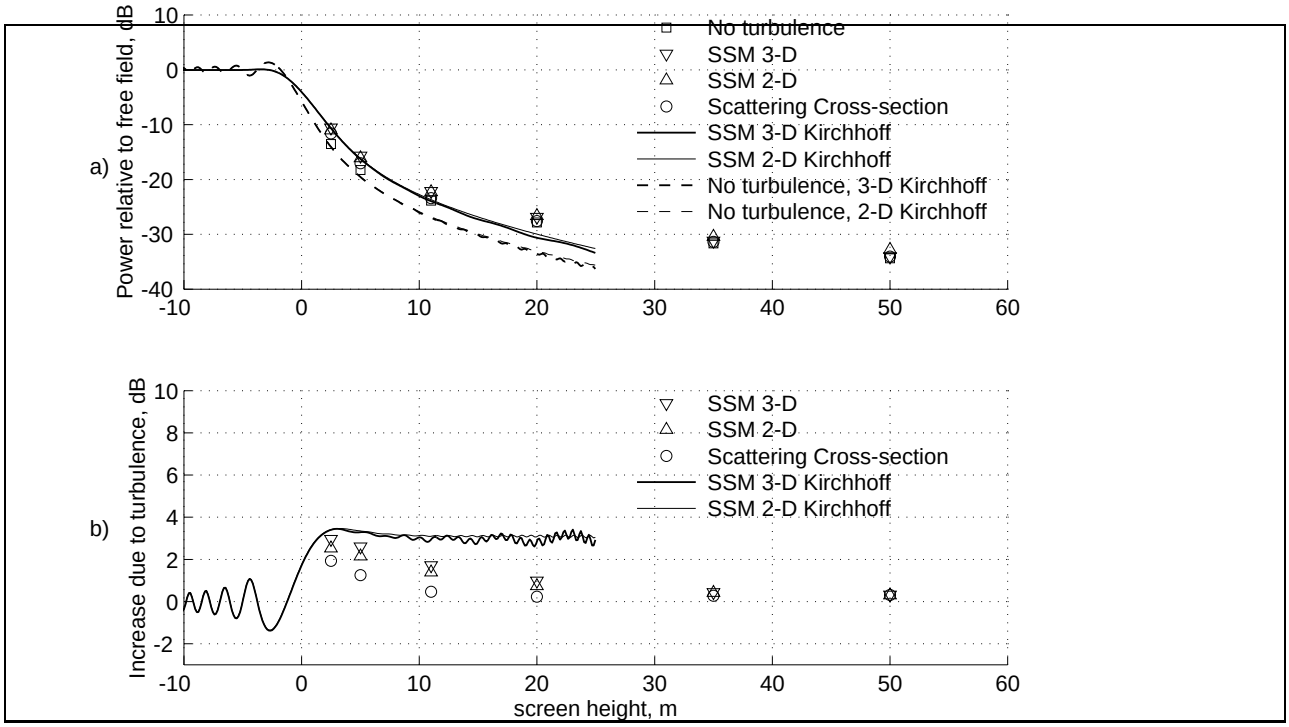

Figure 6. f =500 Hz, d_R =100 m, C_v^2 =5m$^{4/3}$/s^2.

In the Figures 4 through 11, the results are obtained for two frequencies (f =500 Hz and f =1000 Hz), two screen to receiver distances (d_R =100 m and d_R =200 m), and two turbulence strengths (C_v^2 =2.5m$^{4/3}$/s^2 and C_v^2 =5 m$^{4/3}$/s^2). The source to screen distance, d_S, is 20 m for all of the calculations. The results are plotted in dB, as power relative to free field (Figures 4a–11a), and as the increase due to the turbulence (Figures 4b–11b).

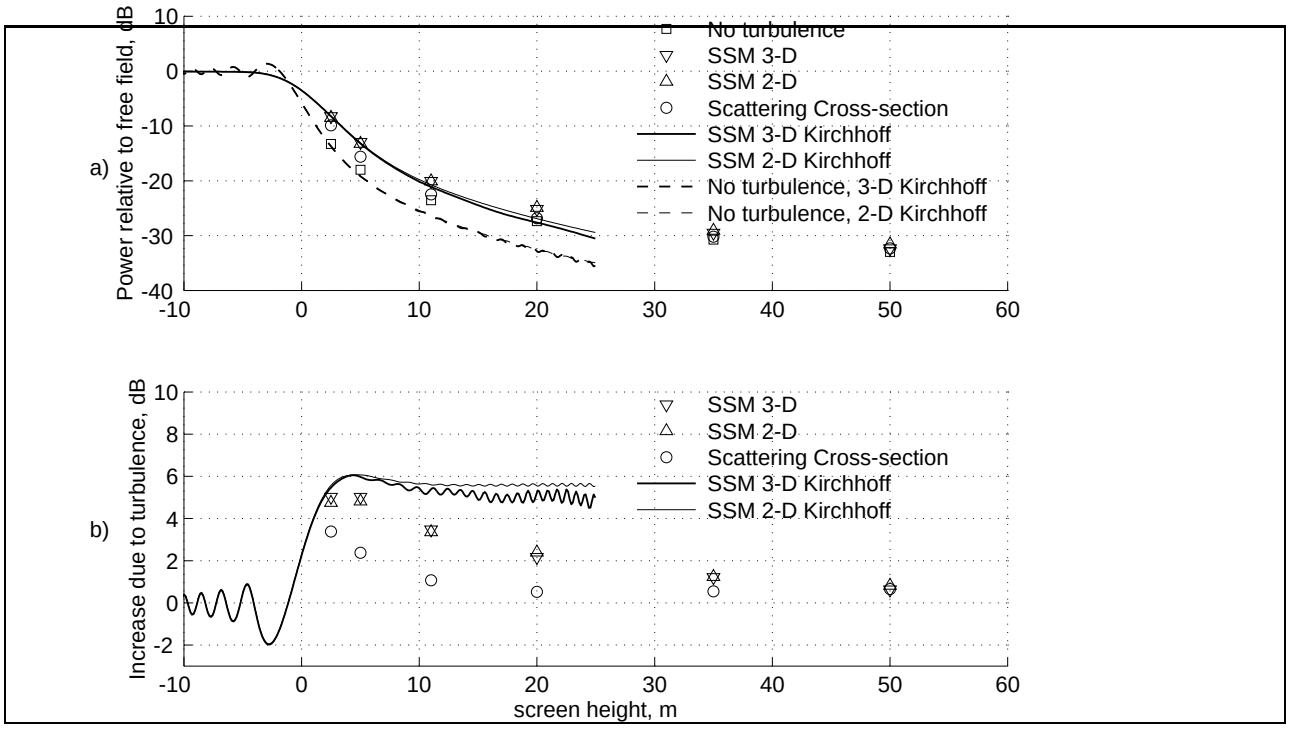

Figure 7. f =500 Hz, d_R =200 m, C_v^2 =5m$^{4/3}$/s^2.

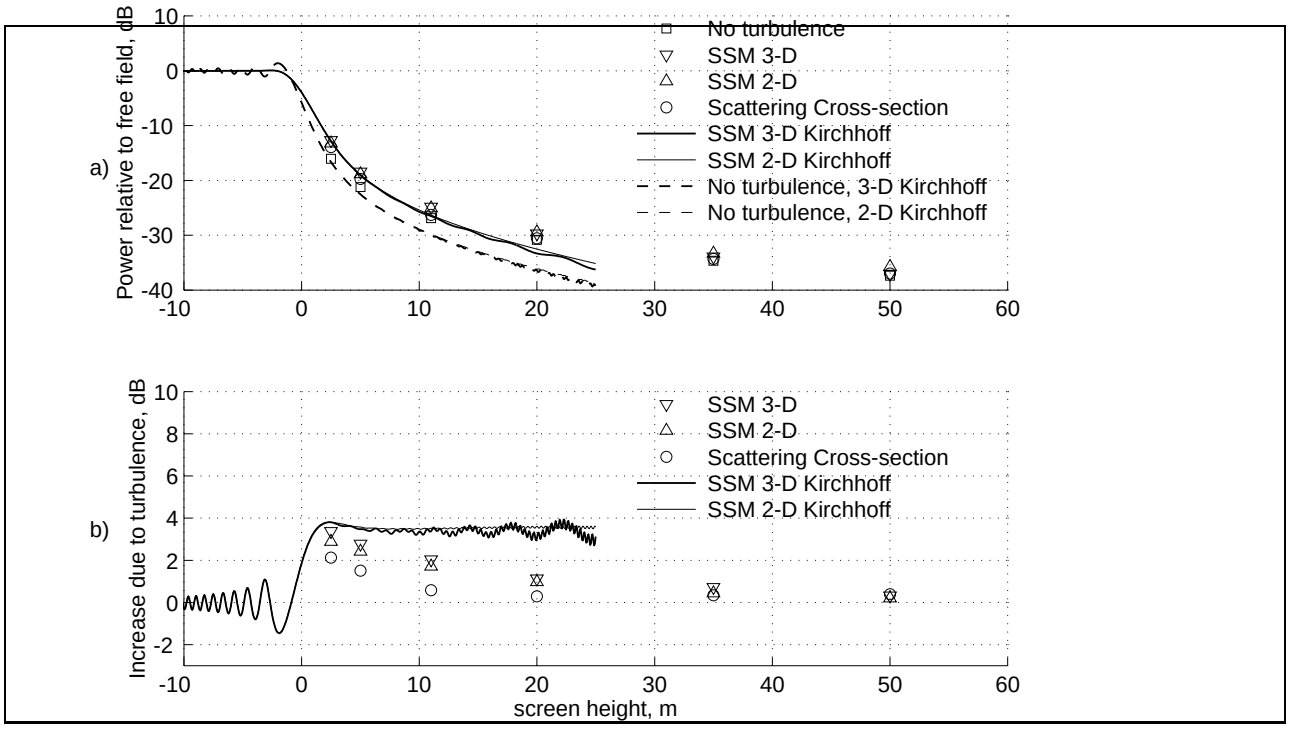

Figure 8. f =1000 Hz, d_R =100 m, C_v^2 =2.5m$^{4/3}$/s^2.

In Figures (4a–11a) the dashed lines show the solutions for a homogeneous atmosphere using the Kirchhoff approximation. The 3-D and the 2-D results are very similar in these examples, except that the 3-D results show unwanted oscillations at greater screen heights. The unwanted oscillations are caused by the finite accuracy in the numerical calculations, due to discretisation and the finite surface, S. These oscillations are present in both the 3-D and the 2-D solutions; since they grow with increasing screen height, it was decided to plot the

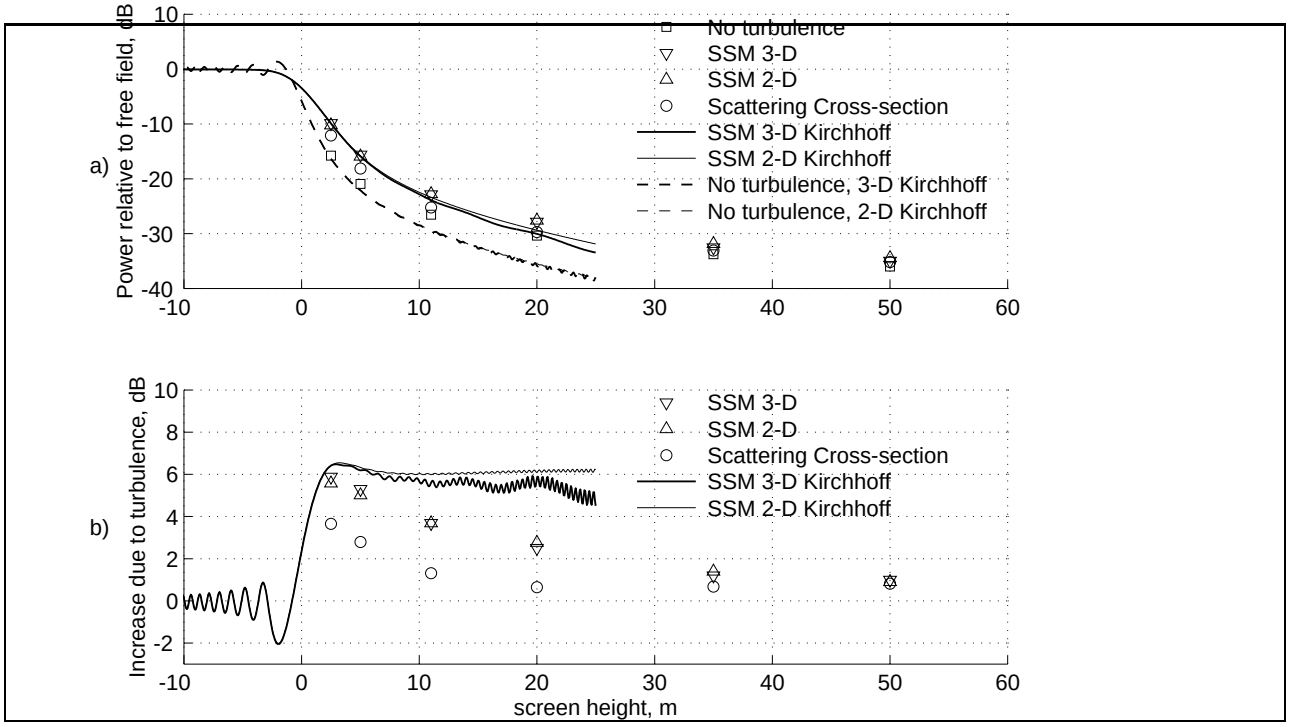

Figure 9. $f = 1000$ Hz, $d_R = 200$ m, $C_v^2 = 2.5\mathrm{m}^{4/3}/\mathrm{s}^2$.

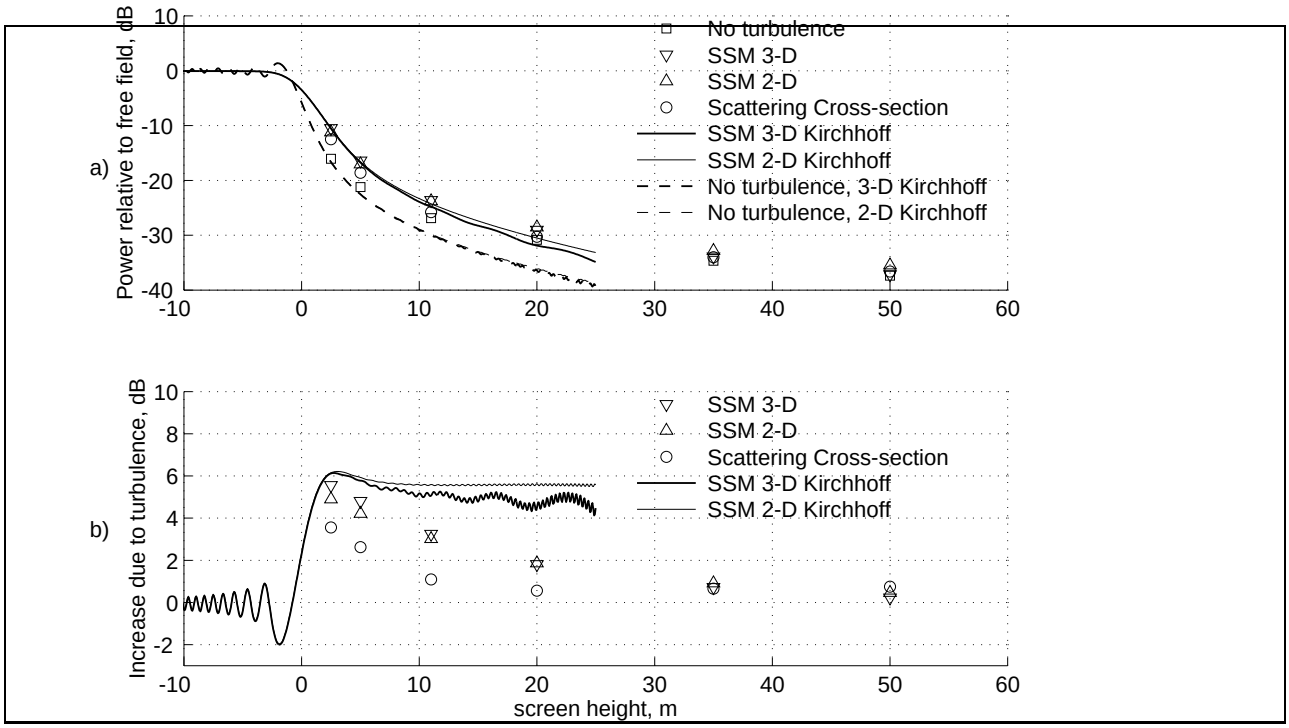

Figure 10. $f = 1000$ Hz, $d_R = 100$ m, $C_v^2 = 5\mathrm{m}^{4/3}/\mathrm{s}^2$.

curves only up to $H = 25$ m. The solid lines are for the turbulence introduced; the 3-D and 2-D results are very similar.

The points when calculating the diffracted field using the UTD, i.e. without the Kirchhoff approximation, are plotted with symbols. The results are shown for 3-D and 2-D calculations with turbulence, for those without turbulence (using the UTD), and for the scattering cross-section method calculations.

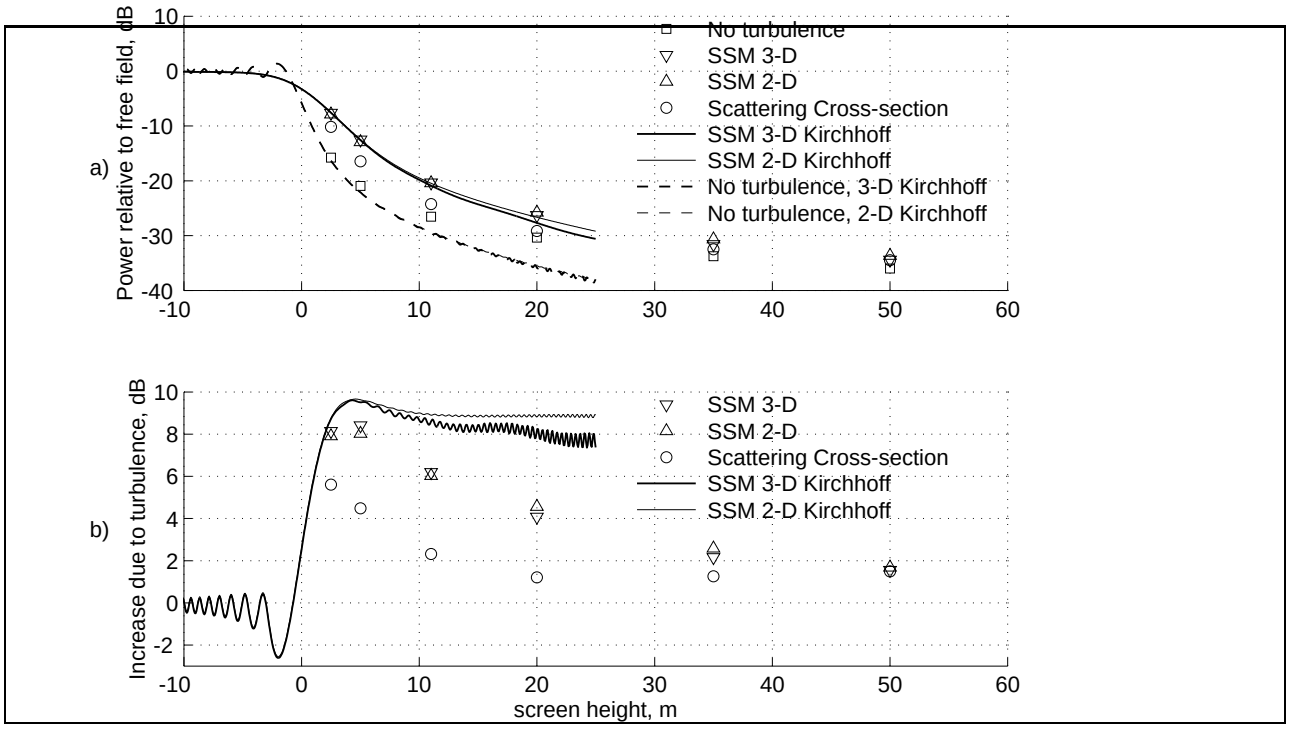

Figure 11. f =1000 Hz, d_R =200 m, C_v^2 =5m$^{4/3}$/s^2.

In Figures (4b–11b) the increase due to the turbulence is shown for the 3-D and the 2-D calculations, with and without the Kirchhoff approximation, as well as for the scattering cross-section method. The unwanted oscillations when using the Kirchhoff approximation are more clearly visible here, and they are stronger for the 3-D calculations than for the 2-D calculations.

The results show a higher sound level when atmospheric turbulence is introduced. As a general trend, the effect of turbulence grows stronger when the frequency, screen to receiver distance, or turbulence strength increases.

For the lower screen heights, the results with and without the Kirchhoff approximation show small differences, as expected. Above $H = 5$ m, however they deviate significantly; using the Kirchhoff approximation is shown to lead to an underestimation of the sound level for the homogeneous examples. Both the 3-D and the 2-D results, when using the exact diffraction velocity, show that the influence of turbulence is weaker for the highest screens. Moreover, the 3-D and 2-D results are very similar throughout all of the calculations. The small differences (about 0.5 dB) indicate that the scattering effect is very similar in both situations.

Although the scattering cross-section method predicts a much weaker influence of turbulence than the SSM, it confirms the trend that there is a range of lower screen heights for which the sound reduction is the most sensitive to turbulence. For the higher screens, where the turbulence influence is weak, the scattering cross-section results are very similar to those for the SSM. It is also shown that for the lower screens the dependence on the turbulence strength is stronger than for the higher screens. Moreover, the screen height at which the maximum influence of turbulence occurs varies with turbulence strength according to the SSM (see Figures 9b and 11b), which is not shown by the scattering cross-section method.

For the higher screens, using the Kirchhoff approximation shows an influence of turbulence that is very weakly linked to the screen height. This is changed if a Gaussian turbulence model is used [6], where a significant turbulence scattering was observed only within a range of lower screen heights. Probably, this contrast

is caused by the fast decay with increasing wave number that the Gaussian model describes, since the smaller scales of the turbulence cause the large angle scattering.

5. Discussion and conclusions

All calculated results show small differences between the 2-D and 3-D situations. This indicates that the sound level increase behind barriers, caused by atmospheric turbulence, can be predicted by using 2-D models in a large variety of situations. The situations studied here are primarily with long screen to receiver distances.

Although the scattering cross-section method predicts a much weaker influence of turbulence than the SSM, it does show the same trend in the results. Since the various situations examined here cover only part of the whole range of those of interest, it is difficult to draw general conclusions about the applicability of the scattering cross-section method.

The Kirchhoff approximation leads to an overestimation of the turbulence influence, for the scenarios studied here; however this might not be so in all situations, e.g. with stronger turbulence and smaller screen to receiver distances.

For an isolated situation with a high enough screen, the scattering contribution due to turbulence decreases faster with increasing screen height than the diffraction contribution. This means that the turbulence affects the sound level within a certain range of screen heights. The range is influenced by geometry, frequency, and turbulence strength.

For a typical traffic noise situation in a city, many noise sources contribute to the noise level in the acoustic shadow of a screen or a house. Since the turbulence influence grows with increasing receiver distance, more distant sources can become more influential.

For future work, it would be of interest to try to include in the model a thick barrier of finite length, a finite impedance ground, a sound speed profile, and an anisotropic and inhomogeneous turbulence.

Acknowledgements

The author wishes to thank Wolfgang Kropp for inspiring discussions and critical reading. This work was financially supported by MISTRA (*Swedish Foundation for Strategic Environmental Research*).

References

[1] Forssén, J. Calculation of noise barrier performance in a turbulent atmosphere by using substitute sources above the barrier. Acustica, Vol. 86, 2000, pp. 269-275.

[2] Daigle, G. A. Diffraction of sound by a noise barrier in the presence of atmospheric turbulence. J. Acoust. Soc. Am., Vol. 71, 1982, pp. 847-854.

[3] Forssén, J. Influence of atmospheric turbulence on sound reduction by a thin, hard screen: A parameter study using the sound scattering cross-section. Proc. 8th Int. Symp. on Long-Range Sound Propagation, The Pennsylvania State University, 1998, pp. 352-364.

[4] Forssén, J. and Ögren, M. Barrier noise-reduction in the presence of atmospheric turbulence: Measurements and numerical modelling. Submitted to Applied Acoustics, November 2000.

[5] Forssén, J. Calculation of sound reduction by a screen in a turbulent atmosphere using the parabolic equation method. Acustica, Vol. 84, 1998, pp. 599-606.

[6] Forssén, J. Calculation of noise barrier performance in a turbulent atmosphere by using substitute sources with random amplitudes. Proc. 9th Int. Symp. on Long-Range Sound Propagation, The Hague, Netherlands, 2000.

[7] Rasmussen, K. B. Model experiments related to outdoor propagation over an earth berm. J. Acoust. Soc. Am., Vol. 96, 1994, pp. 3617-3620.

[8] Kouyoumjian, R. G. and Pathak, P. H. A uniform geometrical theory of diffraction for an edge in a perfectly conducting surface. Proc. IEEE, 62, 1974, pp. 1448-1461.

[9] Kawai, T. Sound diffraction by a many-sided barrier or pillar. Journal of Sound and Vibration, Vol. 79, 1981, pp. 229-242.

[10] L'Espérence, A. and Nicolas, J. and Daigle, G. A. Insertion loss of absorbent barriers on ground. J. Acoust. Soc. Am., Vol. 86, 1989, pp. 1060-1064.

[11] Ostashev, V. E., Brähler, B., Mellert, V. and Goedecke, G. H. Coherence functions of plane and spherical waves in a turbulent medium with the von Karman spectrum of medium inhomogeneities. J. Acoust. Soc. Am., Vol. 104, 1998, pp. 727-737.

[12] Ostashev, V. E. Acoustics in moving inhomogeneous media. E & FN Spon (an imprint of Thomson Professional), London, 1997.

[13] Ishimaru, A. Wave propagation and scattering in random media. IEEE Press (and Oxford University Press, Oxford), New York, 1997.

[14] Karavainikov, V. N. Fluctuations of amplitude and phase in a spherical wave. Sov. Phys. Acoust., Vol. 3, 1956, pp. 175-186.

[15] Forssén, J. Calculation of sound reduction by a screen in a turbulent atmosphere. Report F 98 - 01 (ISSN 0283 - 832X), Chalmers University of Technology, Göteborg, Sweden, 1997.